Soft Matter

Accepted Manuscript

ROYAL SOCIETY OF CHEMISTRY

www.rsc.org/softmatter

Cite this: DOI: 10.1039/c0xx00000x

www.rsc.org/xxxxxx

ARTICLE TYPE

CO_2-switchable multicompartment micelles with segregated corona

Hanbin Liu,[ae] Ying Zhao,[c] Cécile A. Dreiss[d] and Yujun Feng*[ab]

Received (in XXX, XXX) Xth XXXXXXXXX 20XX, Accepted Xth XXXXXXXXX 20XX
DOI: 10.1039/b000000x

CO_2-switchable multicompartment micelles (MCMs) with a segregated corona formed by a purpose-designed ABC triblock copolymer are reported. They can be switched "on" and "off" when sequentially treated with CO_2 and N_2, due to the protonation–deprotonation of the tertiary amine groups along the polymer skeleton.

Multicompartment micelles (MCMs), with a compartmentalized core or corona,[1,2] have attracted unremitting interest[1–11] since the concept was first proposed by Ringsdorf.[12] In addition to the clear fascination of designing elegant structures which mimic the sophistication and high level of compartmentalization, such as eukaryotic cells found in nature,[3] there are obvious advantages in exploiting the distinctive properties of MCMs, in particular for selectively loading two incompatible compounds into the inner subdivided domains and delivering them at the same target site.[2–5]

While the selective storage of different guest molecules in MCMs is an obvious motivation for their synthesis,[4,13] its validation has been limited.[9] More importantly, the selective release of one payload over another has yet to be demonstrated; it would likely require a trigger selectively targeting the various core compartments.[9] CO_2, as an endogenous metabolite, can freely diffuse through cytomembranes without any cytotoxic effect.[14–17] Therefore, developing CO_2 as a stimulus for MCMs holds great promise for biomedical applications. Yuan, Zhao and co-workers,[14–17] for instance, have recently mimicked the deformable behaviour of vesicles in response to CO_2 trigger. Of clear benefit is the reversible nature of the transformation, due to the easy removal of CO_2.[18–23] Nevertheless, switchable MCMs, to the best of our knowledge, have not yet been explored to date.

In this work, we report for the first time CO_2-responsive MCMs with a segregated corona made from a linear ABC triblock copolymer composed of poly(ethylene oxide) (O), poly(2,2,3,4,4,4-hexafluorobutyl methacrylate) (F), and poly(2-(diethylamino)ethyl methacrylate) (E) (Scheme 1a). The water-soluble block "O" stabilizes the micelles in aqueous solution by forming a hydrophilic corona.[3] The fluorinated block "F" is designed to compartmentalize the micellar core into segregated micro-domains, because of the well-known incompatibility between hydro- and fluorocarbons.[1,4,13,24–29] The hydrocarbon segment, "E", has recently been recognized to possess CO_2-sensitivity, and has been used in recyclable catalysts, smart polymer brushes and assemblies for drug delivery.[23,30–33] We originally envisaged that this particular composition would allow the triblock copolymer to self-assemble into MCMs with segregated core domains, since the "E" and "F" blocks are hydrophobic while the "O" block is hydrophilic (before exposure to CO_2). Upon alternating the flow of CO_2 or N_2, the "E" block reversibly changes from a hydrophobic to a hydrophilic state, via a protonation-deprotonation mechanism of the tertiary amines, thus providing a handle for a morphologic transformation. Surprisingly however, the results did not match the expected outcome: the triblock copolymer was found to aggregate into uniform spherical micelles (before the reaction with CO_2) and switch to MCMs with segregated corona (another type of MCMs[1,2]) after treatment with CO_2, as illustrated in Scheme 1b.

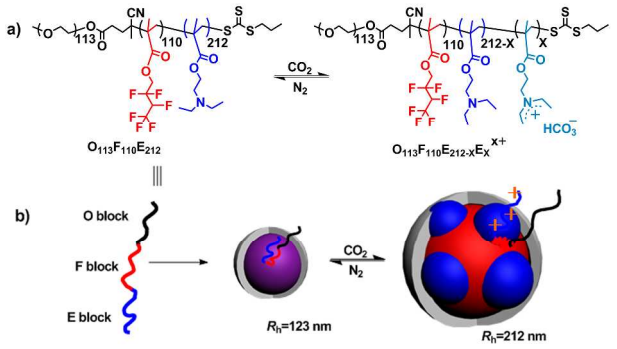

Scheme 1 Molecular structure of the triblock copolymer $O_{113}F_{110}E_{212}$ (a) and schematic representation of the micellar morphology after sequentially bubbling and removing CO_2; (b) triblock copolymer (left); spherical micelle with grey corona formed by the hydrophilic "O" block and purple core formed by hydrophobic "E" and "F" blocks (centre); multicompartment micelle with a red core formed by the "F" block and phase-separated corona, formed of blue charged "E" domains and grey "O" domains (right).

The triblock copolymer $O_{113}F_{110}E_{212}$ was prepared by a two-step reversible addition-fragmentation chain transfer (RAFT) polymerization using a PEO-containing chain transfer agent. The detailed synthesis and characterizations are given in the Supporting Information (Scheme S1, Figs. S1–S4, ESI). After purification, the copolymer was dissolved in *N*,*N*-dimethylformamide (DMF) and dialyzed against deionized water to obtain the aqueous micellar solution.

The CO_2-responsiveness was first confirmed by monitoring the conductivity and pH during successive CO_2 and N_2 bubbling cycles (Fig. 1). Upon CO_2 bubbling, the conductivity of the micellar solution rapidly rises from 22.5 to 56.4 $\mu S \cdot cm^{-1}$, and then gradually increases to the equilibrium value of 62.4 $\mu S \cdot cm^{-1}$. Concurrently, the pH drops from 7.51 to 4.81. Upon N_2 bubbling, CO_2 becomes depleted from the solution, and the conductivity

decreases to 27.4 μS·cm^{-1} while the pH recovers back to 7.20. These variations are remarkably reversible and can be repeated for three cycles without alteration. This trigger benefits from the easy-removal of the unstable bicarbonate salt[34,35] that is produced by the reaction of CO_2 with the tertiary amine groups in the "E" block, thus making it truly reversible, and therefore superior to the more traditional pH trigger (obtained by successive additions of acid and base),[30] where reversibility is affected by the accumulation of by-products.[20]

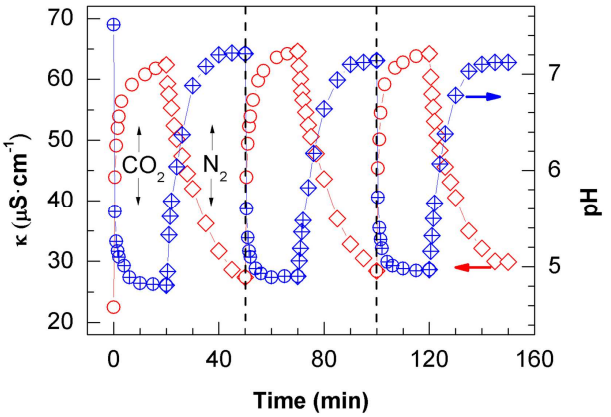

Fig. 1 Conductivity and pH under alternating treatment of CO_2 and N_2 of a 1.0 g·L^{-1} triblock copolymer micellar solution (gas flow is ca. 15 mL·min^{-1}).

In order to rationalise these changes, the protonation of the tertiary amine group was studied next. The pK_a of the triblock copolymer in aqueous solution was established at around 5.9 (Fig. S5), giving a protonation degree (δ, Table S1) of 2% at pH=7.25, and 92% at pH=4.81; the equilibrium value reached upon continuous bubbling of CO_2. A 2% protonation hardly affects the hydrophobicity of the "E" block; however, with 92% of the tertiary amine moieties positively charged, the "E" block becomes hydrophilic, likely to induce substantial structural transitions of the assemblies.[36,37]

Transmission electron microscopy (TEM) was then used to visualise the morphologic changes. Using staining with 0.2 wt% phosphotungstic acid to label the hydrophilic domains, the assemblies appear as spherical aggregates with a light core and a dark outside shell (Fig. 2a) in the absence of CO_2. Noticeably, only some of the spheres exhibit partial segregation (Fig. 2a, pointed by arrows), instead of MCMs with a segregated core, as expected from the original design. This may be related with the incomplete phase separation of the "E" and "F" blocks before reaction with CO_2 (this point is discussed further down).

The aggregates morphologies after exposure and removal of CO_2 were then observed. After treatment with CO_2, the aggregates appear as distinct segregated micro-domains (Figs. 2b), typical of MCMs. Some "hamburgers" (labelled as 1), "reverse hamburgers (2)", "clovers (3)", "footballs (4)" and more complicated structures (5) can be easily distinguished in the TEM image (Figs. 2b). The white regions are attributed to the highly hydrophobic fluorinated "F" block, which cannot be stained by the hydrophilic phosphotungstic acid, while the dark patches within the white regions correspond to the protonated "E" block (Fig. 2b), since phosphotungstic acid can efficiently combine with the pendant positive charged tertiary amines of the "E" block. Upon displacement of CO_2 by N_2, the micro-domains separation disappears and the assemblies revert back to uniform spheres (Fig. 2c).

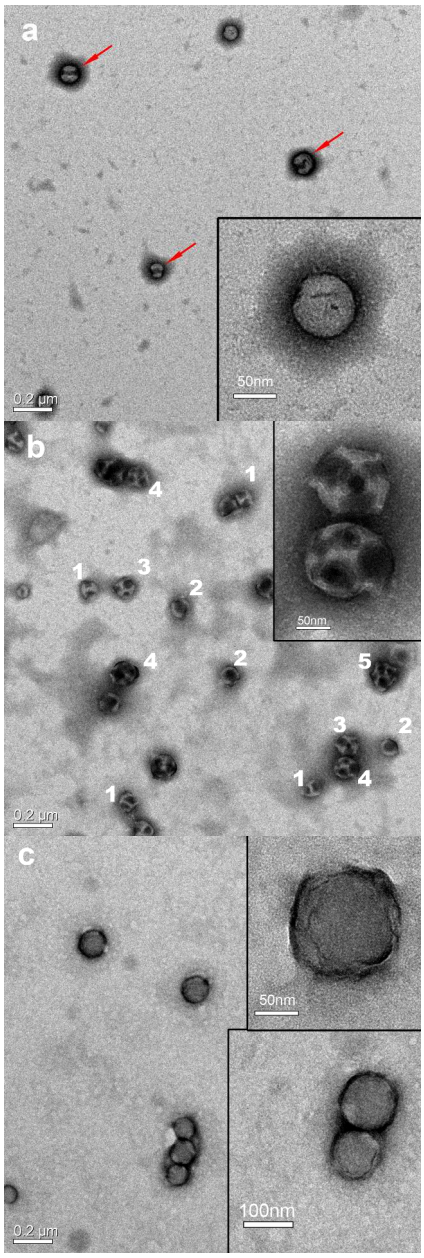

Fig. 2 TEM images of the triblock copolymer assemblies in water stained with 0.2 wt% phosphotungstic acid. (a) before bubbling CO_2; (b) after bubbling CO_2; the different numbers distinguish between different types of MCMs: "hamburgers"(1), "reverse hamburgers" (2), "clovers" (3), "footballs" (4) and more complex structures (5). (c) after CO_2 removal by bubbling N_2. The polymer concentration was fixed at 1.0 g·L^{-1}. Scale bars in (a), (b) and (c) are 0.2 μm (main picture) and 50 nm (insets, except bottom one at 100 nm).

Since the phosphotungstic acid can only effectively stain the charged "E" block, we also observed the aggregates with CO_2 treatment after staining with RuO_4 vapor for 8 min, which would stain the hydrophobic "F" block rather than the "E" block. Müller and coworkers,[1] for instance, have been able to visualize fluorinated blocks as dark regions by RuO_4 staining. As shown in Fig. 3, various MCM structures were also observed, including

"hamburgers" (a, b), "footballs" (c, d) and higher-order structures (d, e). Compared with the images stained with phosphotungstic acid, the dark micro-domains should be formed by the fluorinated block "F", corresponding to the white regions in the sample stained with phosphotungstic acid (Fig. 2b). Instead, the light regions should now be the charged "E" domains, while they appear dark in Fig. 2b. The combination of two staining methods for the "E" and "F" blocks in TEM images confirms their phase segregation into microdomains in the presence of CO_2.

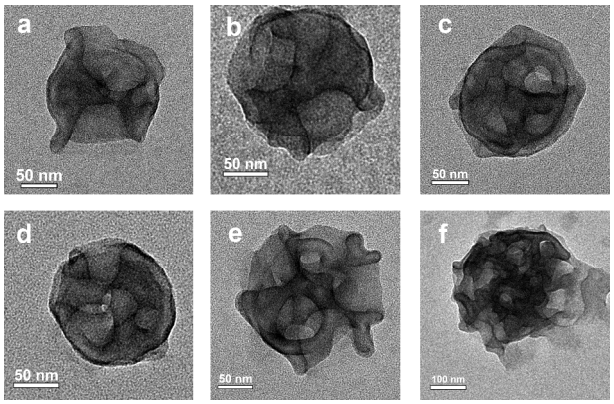

Fig. 3 TEM micrographs of the triblock copolymer assemblies (1.0 g·L^{-1}) in water stained with RuO_4 in the presence of CO_2. Scale bars: 100 nm (f); 50 nm (others).

As a final confirmation of the MCMs structures, cryogenic transmission electron microscopy (cryo-TEM) was employed to ensure the lack of artifacts linked to staining.[9] Upon exposure to CO_2, segregated "F" and "E" domains are clearly distinguished (Fig. S7a–h) with dark, electron-rich fluorocarbon "F" blocks and lighter charged "E" blocks. Some of the aggregates appear as "hamburgers" (c, d), "clovers" (b, d, e) and "footballs" (f, g, h), in good agreement with the TEM observation (Fig. 2b and Fig. 3). Upon depletion of CO_2 by N_2, the MCMs convert back to smooth spherical micelles without visible segregated micro-domains (Fig. S7i), again concurring with TEM observations (Fig. 2c). Noticeably, upon re-bubbling of CO_2, the MCMs re-appear (Fig. S7j–k), showing the reversibility of the morphologic transformation.

In order to ensure that the observed structures are not caused by the aggregation of vesicles[38], we further employed SEM measurements. Zhou[39] and Zhao[17] have been able to observe holes in vesicles with scanning electron microscope (SEM). We also performed SEM measurement after drying several drops of a micellar solution on a clean mica plate. No particles with holes were found in the SEM images (Fig. S8); instead, they all appeared as plain spheres. Furthermore, a dissipative particle dynamics (DPD) simulation on the self-assemblies before and after treatment with CO_2 was performed, to theoretically confirmMCM formation (details in ESI). A model ABC linear triblock copolymer $A_{12}B_6C_{10}$ was constructed to mimic the triblock copolymer $O_{113}F_{110}E_{212}$ synthesized in this work. Before bubbling CO_2, incomplete phase separation results in spherical micelles (Fig. S10). After reaction with CO_2, the repulsion parameter α_{BC} changes from 30 (before bubbling CO_2) to 75 (Tables S2 and S3), thus resulting in significant phase separation of the "F(B)" block (red) and charged "E(C)" block (green) as shown in Fig. 4a, b and c. From the cross-section of the aggregate (Fig. 4d), a "clover" was found with three patches formed by the "E(C)" block (green), in agreement with the TEM and cryo-TEM observations. The simulations thereforesupports the experimental observations, by theoretically demonstrating the formation of MCMs.

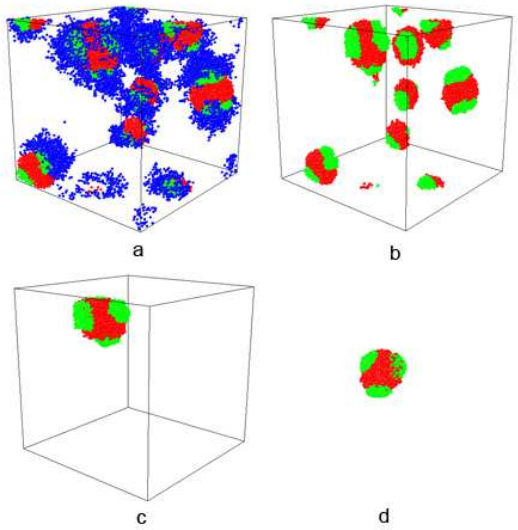

Fig. 4 Morphologies of the multicompartment micelles self-assembled from triblock copolymer in water after bubbling CO_2 (a): triblock copolymer $A_{12}B_6C_{10}$ self-assembly in water, block A: blue, block B: green, block C: red; (b) self-assembly of the core of the triblock copolymer $A_{12}B_6C_{10}$; (c) core of one micelle; (d) cross-section of the micellar core (c).

Atomic force microscopy (AFM) measurements were then carried out to determine the size of the micelles, and in particular the hydrophilic "O" block, since it cannot be directly visualized by TEM or cryo-TEM. As exhibited in Fig. 5, the morphology of the aggregates, both after bubbling CO_2 and N_2, appears spherical. However, cross-sectional analysis from the base-line width reveals a radius of approximately 390 nm after bubbling CO_2 (Fig. 5a) against 130 nm after removal of CO_2 by bubbling N_2 (Fig. 5b), though these values might be larger than the real sizes because of the flattening of the spheres. Dynamic light scattering (DLS) measurements corroborate this size discrepancy (Fig. 5c), showing a hydrodynamic radius (R_h) of 212 ± 8 nm in the presence of CO_2, and only 123 ± 5 nm after the replacement of CO_2 by N_2, thus confirming a shrinkage of the micelles to half their size, in good agreement with AFM analysis. More importantly, this process is fully reversible: when CO_2 is bubbled again, the micellar size reverts back to 210 ± 6 nm (Fig. 4c), very close to the size obtained after first treatment by CO_2.

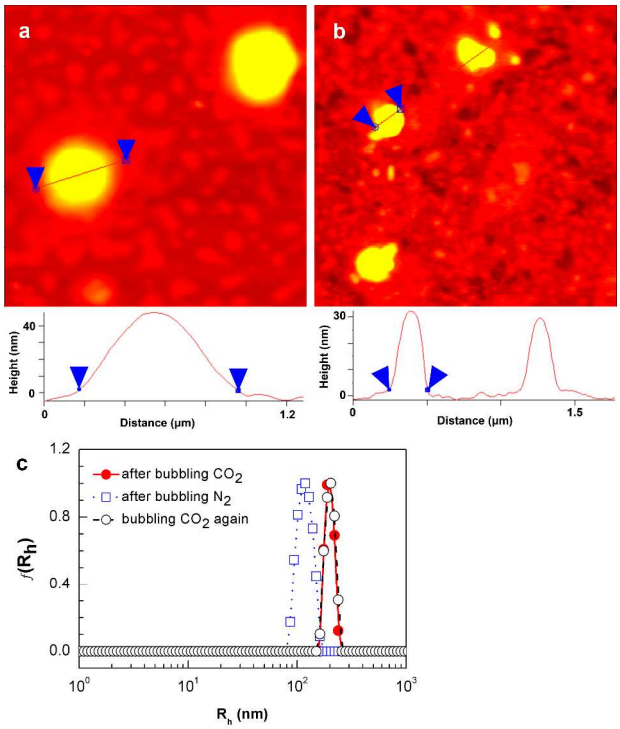

Fig. 5 AFM observation (a, after reaction with CO_2; b, after removal of CO_2) and DLS measurement (c) of the triblock copolymer aggregates with polymer concentration of 1.0 g·L^{-1}.

Based on the above findings, we propose a mechanism to rationalize the morphological changes. First of all, the appearance of the triblock copolymer micelles in the absence of CO_2 as homogeneous spheres (Figs. 2a, 2c, and 3b) – either the original micelles before CO_2 bubbling or after the removal of CO_2 by N_2 bubbling – is puzzling, since a segregation between hydro- and fluorocarbons leading to a compartmentalization of the core would have been expected. Laschewsky and coworkers[28] was able to confirm the phase separation in MCM using differential scanning calorimetry (DSC). Here, the thermal behavior of the triblock copolymer $O_{113}F_{110}E_{212}$ and its two diblock precursors, $O_{113}E_{212}$ and $O_{113}F_{110}$ were also studied by DSC (see ESI), showing distinct glass transition temperatures (T_g) for the "O", "E" and "F" blocks at −70 °C, 45 °C and 68 °C, respectively. Nevertheless, an additional peak at 85 °C is detected in the DCS curve of the triblock copolymer $O_{113}F_{110}E_{212}$, indicating the coexistence of three microphases of each polymer block.[28] This suggests that the macro-phase separation between the "E" and "F" blocks is incomplete when the "E" block is in the hydrophobic state – i.e. in the absence of CO_2 - thus inducing the formation of uniform spheres rather than MCMs with a compartmentalized core. Upon exposure to CO_2, the pendant tertiary amine groups in the "E" block become protonated (from 2% to 92%), stretching into water due to the strong electrostatic repulsions, thus resulting in phase segregation of the three blocks. The fluorinated "F" block remains highly hydrophobic and forms the core, while the hydrophilic "E" and "O" block form a segregated corona, thus "switch on" the MCMs, as depicted in Scheme 1. In addition, the fluorocarbon core itself does not display the typical spherical shape but appears as a higher order structure, due to the intensive repulsions between the charged "E" blocks which are bonded to the "F" blocks. This finding explains why the size increases during the morphologic transition.

In conclusion, we report here the first example of MCMs with a segregated corona, which can reversibly be switched "on" and "off" by alternately bubbling and displacing CO_2: upon exposure to CO_2, the triblocks spontaneously assemble into MCMs; when CO_2 is removed by N_2, they revert back to uniform spherical micelles. The protonation–deprotonation mechanism of the tertiary amine groups along the "E" block is responsible for this reversible morphologic transition. CO_2 offers many advantages as a trigger, in particular a lack of accumulation of contaminants, and therefore, provides a reversible process over many cycles. To the best of our knowledge, this represents a step-increase in sophistication in the design of MCMs. In particular, these CO_2-switchable MCMs open the door to selective, finely controlled uptake and delivery of two or more drugs in only one nano-vehicle.

Acknowledgements

This work was financially supported by the National Natural Science Foundation of China (21273223, 21173207) and Distinguished Youth Fund from Science and Technology Department of Sichuan Province (2010JQ0029). Ying Zhao acknowledges the financial support from National Natural Science Foundation of China (21203179) and Fundamental Research Funds for the Central Universities (DC13010219. B).

Notes and references

[a] *Chengdu Institute of Organic Chemistry, Chinese Academy of Sciences, Chengdu 610041, P. R. China*
[b] *Polymer Research Institute, State Key Laboratory of Polymer Materials Engineering, Sichuan University, Chengdu 610065, P. R. China*
E-mail: yjfeng@scu.edu.cn
[c] *Institute of Nano-Photonics, School of Physics and Materials Engineering, Dalian Nationalities University, Dalian 116600, P. R. China*
[d] *Institute of Pharmaceutical Science, 150 Stamford Street, King's College London, UK SE1 9NH*
[e] *University of the Chinese Academy of Sciences, Beijing 100049, P. R. China*

† Electronic Supplementary Information (ESI) available: polymerization and characterization of block copolymers, pK_a titration, SEM images and cryo-TEM photographes, DSC results and DPD simulation. See DOI: 10.1039/b000000x/

1. B. Fang, A. Walther, A. Wolf, Y. Xu, J. Yuan and A. H. E. Müller, *Angew. Chem. Int. Ed.*, 2009, **48**, 2877–2880.
2. A. H. Gröschel, F. H. Schacher, H. Schmalz, O. V. Borisov, E. B. Zhulina, A. Walther and A. H. E. Müller, *Nat. Commun.*, 2012, **3**, 710.
3. Z. Li, E. Kesselman, Y. Talmon, M. A. Hillmyer and T. P. Lodge, *Science*, 2004, **306**, 98–101.
4. T. P. Lodge, A. Rasdal, Z. Li and M. A. Hillmyer, *J. Am. Chem. Soc.*, 2005, **127**, 17608–17609.
5. S. Kubowicz, J.-F. Baussard, J.-F. Lutz, A. F. Thünemann, H. von Berlepsch and A. Laschewsky, *Angew. Chem. Int. Ed.*, 2005, **44**, 5262–5265.
6. H. Cui, Z. Chen, S. Zhong, K. L. Wooley and D. J. Pochan, *Science*, 2007, **317**, 647–650.
7. L. Nie, S. Liu, W. Shen, D. Chen and M. Jiang, *Angew. Chem. Int. Ed.*, 2007, **46**, 6321–6324.
8. L. Cheng, G. Z. Zhang, L. Zhu, D. Y. Chen and M. Jiang, *Angew. Chem. Int. Ed.*, 2008, **47**, 10171–10174.
9. A. O. Moughton, M. A. Hillmyer and T. P. Lodge, *Macromolecules*, 2012, **45**, 2–19.
10. J. Mao, P. Ni, Y. Mai and D. Yan, *Langmuir*, 2007, **23**, 5127–5134.

11. H. Zhang, P. Ni, J. He and C. Liu, *Langmuir*, 2008, **24**, 4647–4654.
12. A. Laschewsky, *Curr. Opin. Colloid Interface Sci.*, 2003, **8**, 274–281.
13. J. N. Marsat, M. Heydenreich, E. Kleinpeter, H. V. Berlepsch, C. Bottcher and A. Laschewsky, *Macromolecules*, 2011, **44**, 2092–2105.
14. Q. Yan, R. Zhou, C. Fu, H. Zhang, Y. Yin and J. Yuan, *Angew. Chem. Int. Ed.*, 2011, **50**, 4923–-4927.
15. Q. Yan, J. Wang, Y. Yin and J. Yuan, *Angew. Chem. Int. Ed.*, 2013, **52**, 5070–5073.
16. Q. Yan and Y. Zhao, *Angew. Chem. Int. Ed.*, 2013, **52**, 9948–9951.
17. Q. Yan and Y. Zhao, *J. Am. Chem. Soc.*, 2013, **135**, 16300–16303.
18. Y. Liu, P. G. Jessop, M. Cunningham, C. A. Eckert and C. L. Liotta, *Science*, 2006, **313**, 958–960.
19. Z. Guo, Y. Feng, Y. Wang, J. Wang, Y. Wu and Y. Zhang, *Chem. Commun.*, 2011, **47**, 9348–9350.
20. P. G. Jessop, S. M. Mercer and D. J. Heldebrant, *Energy Environ. Sci.*, 2012, **5**, 7240–7253.
21. Z. Guo, Y. J. Feng, S. He, M. Qu, H. Chen, H. Liu, Y. F. Wu and Y. Wang, *Adv. Mater.*, 2013, **25**, 584–590.
22. S. Lin and P. Theato, *Macromol. Rapid Commun.*, 2013, **34**, 1118–1133.
23. A. J. Morse, S. P. Armes, K. L. Thompson, D. Dupin, L. A. Fielding, P. Mills and R. Swart, *Langmuir*, 2013, **29**, 5466–5475.
24. Z. B. Li, M. A. Hillmyer and T. P. Lodge, *Langmuir*, 2006, **22**, 9409–9417.
25. Z. B. Li, M. A. Hillmyer and T. P. Lodge, *Macromolecules*, 2006, **39**, 765–771.
26. C. Liu, M. A. Hillmyer and T. P. Lodge, *Langmuir*, 2008, **24**, 12001–12009.
27. H. v. Berlepsch, C. Bottcher, K. Skrabania and A. Laschewsky, *Chem. Commun.*, 2009, **0**, 2290–2292.
28. K. Skrabania, A. Laschewsky, H. von Berlepsch and C. Bottcher, *Langmuir*, 2009, **25**, 7594–7601.
29. K. Skrabania, H. von Berlepsch, C. Bottcher and A. Laschewsky, *Macromolecules*, 2010, **43**, 271–281.
30. S. Kumar, X. Tong, Y. Dory, M. Lepage and Y. Zhao, *Chem. Commun.*, 2013, **49**, 90-92.
31. J. Zhang, D. Han, H. Zhang, M. Chaker, Y. Zhao and D. Ma, *Chem. Commun.*, 2012, **48**, 11510–11512.
32. D. Han, X. Tong, O. Boissière and Y. Zhao, *ACS Macro Lett.*, 2011, **1**, 57–61.
33. B. Yan, D. H. Han, O. Boissiere, P. Ayotte and Y. Zhao, *Soft Matter*, 2013, **9**, 2011–2016.
34. Y. Zhang, Y. Feng, J. Wang, S. He, Z. Guo, Z. Chu and C. A. Dreiss, *Chem. Commun.*, 2013, **49**, 4902–4904.
35. Y. Zhang, Z. Chu, C. A. Dreiss, Y. Wang, C. Fei and Y. Feng, *Soft Matter*, 2013, **9**, 6217–6221.
36. D. E. Discher and A. Eisenberg, *Science*, 2002, **297**, 967–973.
37. D. E. Discher and F. Ahmed, *Annu. Rev. Biomed. Eng.*, 2006, **8**, 323–341.
38. M. Zhang, Y. Hu, Y. Hassan, H. Zhou, K. Moozeh, G. D. Scholes and M. A. Winnik, *Soft Matter*, 2013, **9**, 8887–8896.
39. Y. Liu, C. Yu, H. Jin, B. Jiang, X. Zhu, Y. Zhou, Z. Lu and D. Yan, *J. Am. Chem. Soc.*, 2013, **135**, 4765–4770.

Graphical and Textual Abstract of Contents

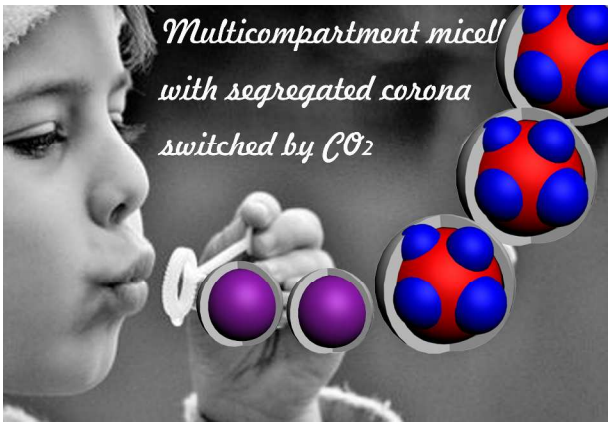

Multicompartment micelles (MCMs) with segregated corona formed from a specifically-tailored linear ABC triblock copolymer can be switched "on" and "off" when sequentially treated with CO_2 and N_2.